Hindawi Publishing Corporation
Journal of Computational Medicine
Volume 2014, Article ID 504656, 7 pages
http://dx.doi.org/10.1155/2014/504656

Research Article

Validation of Shape Context Based Image Registration Method Using Digital Image Correlation Measurement on a Rat Stomach

Donghua Liao,[1,2] Peng Wang,[3] Jingbo Zhao,[1,2] and Hans Gregersen[4,5]

[1] *GIOME Academia, Institute of Clinical Medicine, Aarhus University Hospital, 8200 Aarhus, Denmark*
[2] *Mech-Sense, Department of Gastroenterology and Surgery, Aalborg University Hospital, 9000 Aalborg, Denmark*
[3] *Department of Mechanical and Manufacturing Engineering, Aalborg University, 9220 Aalborg, Denmark*
[4] *College of Bioengineering, Chongqing University, Chongqing 400050, China*
[5] *The GIOME Institute, Dubai, UAE*

Correspondence should be addressed to Donghua Liao; liao.donghua@ki.au.dk

Received 7 October 2013; Revised 8 December 2013; Accepted 9 December 2013; Published 8 January 2014

Academic Editor: Jackie Wu

Recently we developed analysis for 3D visceral organ deformation by combining the shape context (SC) method with a full-field strain (strain distribution on a whole 3D surface) analysis for calculating distension-induced rat stomach deformation. The surface deformation detected by the SC method needs to be further verified by using a feature tracking measurement. Hence, the aim of this study was to verify the SC method-based calculation by using digital image correlation (DIC) measurement on a rat stomach. The rat stomach exposed to distension pressures 0.0, 0.2, 0.4, and 0.6 kPa were studied using both 3D DIC system and SC-based image registration calculation. Three different surface sample counts between the reference and the target surfaces were used to gauge the effect of the surface sample counts on the calculation. Each pair of the surface points between the DIC measured target surface and the SC calculated correspondence surface was compared. Compared with DIC measurement, the SC calculated surface had errors from 5% to 23% at pressures from 0.2 to 0.6 kPa with different surface sample counts between the reference surface and the target surface. This indicates good qualitative and quantitative agreement on the surfaces with small dissimilarity and small sample count difference between the reference surface and the target surface. In conclusion, this is the first study to validate the 3D SC-based image registration method by using unique tracking features measurement. The developed method can be used in the future for analysing scientific and clinical data of visceral organ geometry and biomechanical properties in health and disease.

1. Introduction

Identifying corresponding points between two configurations is a common problem in medical image processing. Point matching-based surface registration using 3D shape context (SC) has recently emerged as an alternative to intensity-based nonlinear registration. The major contribution of SC lies in the global shape characterization at a local level for each single point. The point matching is based on 3D shape descriptors that characterize the shape of each point based on histograms of the distribution of points around them. Corresponding points on similar shapes will have similar shape contexts. In comparison to other point matching techniques, SC do not require an equal number of points for the shapes to be compared or segments with specific geometrical configurations [1, 2].

Studies on lung and cortical surfaces demonstrated that the SC matching approach-based nonlinear registration method is a well-suited method for a variety of soft tissue organ surfaces [1, 3–8]. Recently we developed a 3D SC-based nonlinear image registration by combining the image registration method with a full-field strain (strain distribution on a whole 3D surface) analysis for calculation of distension-induced rat stomach deformation [9]. Our study showed the dependency of the surface deformation estimation on the surface matching quality. Consequently, for exploring the developed method on estimations of *in vivo* visceral organs surface deformation, validation of the SC-based surface point

matching is needed. Existing validation tests of 3D SC method were limited in (1) the matching experiments that were on synthetically transformed data (the target surface for the registration was mathematically transformed from a reference surface [5, 7, 8]), (2) the equal number of surface points that was selected between the reference surface and the target surface [7], and (3) only few surface points were selected manually for comparisons between the target surface and SC method calculated correspondence surface [2]. The configuration of the visceral organ changes with large deformation due to nonlinear tissue mechanical properties. Moreover, *in vivo* deformation of the visceral organ is location and orientation dependent due to the diseases caused tissue remodelling or heterogeneous tissue properties. Hence, *in vivo* movement or deformation in the visceral organs undergoes a complex and irregular configuration change, and it is difficult to map the deformed surface through a transformation from a reference surface.

From 3D surface reconstruction aspects of view, it is difficult to maintain the equal number of surface points on surfaces that are reconstructed from images at various geometric or mechanical states. Therefore, it is necessary to validate the 3D SC method by comparing if the calculated correspondence surface is identical to the measured target surface at each surface point. Only a feature tracking measurement, for example, 3D digital image correlation (DIC) photogrammetry, is able to follow each surface point between the reference surface and the target surfaces. DIC measurement obtains the deformation of a surface by comparison of digital images of the undeformed and deformed configuration shapes. The assumption is that there is direct correspondence between the motions of points in the image and motions of points on the object. With the use of two CCD cameras, the DIC measurement is becoming a popular and widely used tool for 3D deformation analysis [10]. Therefore, DIC measurement is an excellent tool for verifying the SC-based 3D model registrations *in vitro* [11].

In this study, a rat stomach exposed to distension pressures 0.0, 0.2, 0.4, and 0.6 kPa was investigated by the DIC measurement for capturing the correspondence surface points during the distensions. In the meantime, the correspondence surface points between pressure 0.0 and pressures 0.2, 0.4, and 0.6 kPa were estimated by SC method, in which the DIC measured surface at pressure 0.0 was used as a reference surface, and surfaces at pressures 0.2, 0.4, and 0.6 kPa were used as the target surfaces. The target surfaces were registering to the reference surface and the point-by-point correspondence between the reference surface and the target surface was established. The purpose of this study was to verify the surface point matching calculated by SC method from the DIC measurement on a distended rat stomach.

2. Materials and Methods

In this study, a rat stomach with marked black dots on the outer surface was used as an example to verify the accuracy of the 3D shape context- (SC-) based nonrigid image registration. The rat stomach was selected because, in our recent study, the 3D SC method combined with a full-field strain analysis method was introduced, and full-field strain analysis on a rat gastric model with distension pressures from 0.1 kPa to 0.8 kPa was obtained. We are hereby using DIC measurement to validate the 3D SC method described in our previous study [9].

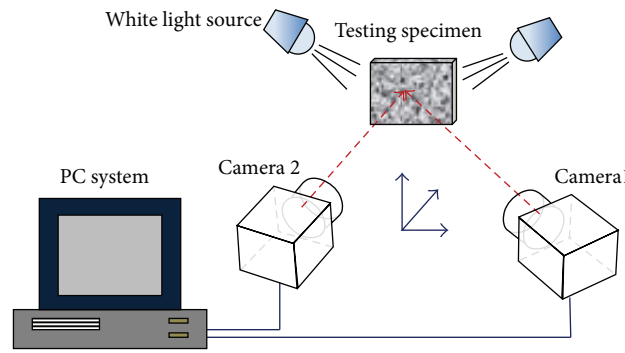

Figure 1: A schematic plot of DIC testing setup.

2.1. Stomach Sample. The stomach of a Wistar rat weighing 300 g was used in this study. The rat was anaesthetised with Hypnorm 0.5 mg and Dormicum 0.25 mg per 100 g body weight. Following laparotomy, the whole stomach with the distal part of the oesophagus and the proximal part of the duodenum was excised. The stomach was rinsed with saline solution introduced into the lumen through the distal oesophagus. The rat was killed by a CO_2 inhalation overdose after the stomach was taken out of the abdominal cavity in accordance with guidelines and approval from the Danish Committee for Animal Experimentation. The experiment was conducted at room temperature.

2.2. Experimental Setup and Procedure. The stomach surface was gently dried and cleaned by tissue papers and was sprayed with white paint for making a white background. After a few seconds, the outer surface was sprayed with black dye to mark the stomach surface in a random dot pattern. The stomach was suspended (greater curvature down) in an organ bath by fixing the oesophageal end and the duodenal end vertically to a bar above the organ bath for avoiding rigid movement and rotation of the stomach during the distensions. The bar was then lowered to completely submerge the stomach into the organ bath. The organ bath was filled with saline solution. The duodenal end was closed after the pressure equilibration and the oesophageal end was connected via a tube to a fluid container containing saline solution. The container was used for applying static gastric luminal pressures of 0.0, 0.2, 0.4, and 0.6 kPa. Five minutes were allowed for equilibration at each pressure level.

The stomach was photographed at each pressure level using a 3D DIC system (ARAMIS 4 M, GOM GmbH, Germany) (Figure 1). A basic idea of this technique is to determine 3D coordinates of the points from a pair of pictures with two different cameras in same magnifications. The configuration of these two cameras was obtained by a calibration process with the aid of a calibration object. 3D DIC system measures the complete 3D surface displacement

fields on curved or planar specimens, with accuracy on the order of ±0.01 pixels for the in-plane components and $Z/50000$ in the out-of-plane component, where Z is the distance from the object to the camera [9, 12]. In the present study, two cameras with 50 mm lenses and a resolution of 2048 × 2048 pixel2 were used to capture pairs of images at each distension pressure. The distance from the stomach to the camera was about 50 cm. The stomach surface with pressure of 0.0 kPa was used as the reference configuration. Each image was divided into many small computational units called facets or subsets. The detected stomach surface was reconstructed from the 3D coordinates of the centre of each facet. The distension which caused surface outwards displacement at each surface point was denoted as

$$D_i = \sqrt{\left(x_{i\_\mathrm{DIC}} - X_{i\_\mathrm{DIC}}\right)^2 + \left(y_{i\_\mathrm{Dic}} - Y_{i-\mathrm{Dic}}\right)^2 + \left(z_{i\_\mathrm{Dic}} - Z_{i\_\mathrm{Dic}}\right)^2}, \quad (1)$$

where x, y, z and X, Y, Z are surface point coordinates in x, y, and z directions at the deformed state and the reference state, i_DIC is the surface points on the DIC measured surface, and $i = 1, 2, 3 \ldots n$ is number of the surface points.

2.3. SC Method-Based Calculations. The shape context (SC) is a shape descriptor that for a single surface captures the distribution of points over relative positions of the global shape points. In our recent study, we have extended the 2D SC to 3D and have developed the 3D SC by a combination to a 3D full-field surface strain calculation [9]. Details about SC method are described in Appendices A and B.

Based on the DIC measured surface at pressure 0.0 kPa, three references surfaces for SC method were reconstructed as reference surface 1 (RS 1), the same surface as that detected by DIC measurement; reference surface 2 (RS 2), the same surface as reference surface 1, but resampling with 90% surface sample counts of the RS 1 (selecting 9 surface points in every 10 surface points); and reference surface 3 (RS 3), the same surface as reference surface 1, but resampling with 80% surface sample counts of the RS 1 (selecting four surface points in every five surface points). The DIC measured surfaces at pressures 0.2, 0.4, and 0.6 kPa were used as three target surfaces. For each reference surface, all three target surfaces were registering to align with the reference surface, and the point-by-point correspondence between the reference surface and the target surface was established by using the SC method-based nonlinear image registration analysis.

2.4. Accuracy of the SC Method-Based Calculations. The accuracy of the SC method was described as, with the same reference surface, the deviation of each pair of surface point between the DIC measurement (target surface) and the SC calculated correspondence surface as

$$\varepsilon_i\% = 100 * \frac{\sqrt{\left(x_{i\_\mathrm{DIC}} - x_{i\_\mathrm{SC}}\right)^2 + \left(y_{i\_\mathrm{Dic}} - y_{i\_\mathrm{SC}}\right)^2 + \left(z_{i\_\mathrm{Dic}} - z_{i\_\mathrm{SC}}\right)^2}}{D_i}, \quad (2)$$

where x, and y, z are surface point coordinates in x, y, and z directions at the deformed state; i_DIC and i_SC are the surface points on the DIC measured surface and the SC calculated surface; D_i is the DIC measured displacement on the surface point as that presented in (1); $i = 1, 2, 3 \ldots n$ is number of the surface points; and n is equal to the surface sample counts at the selected reference surface.

2.5. Statistical Analysis. Data are expressed as means ± SD. Two-way ANOVA was used to distinguish difference in distension pressure 0.2, 0.4, and 0.6 kPa and with three reference surfaces. Differences were considered statistically significant if $P < 0.05$. All analyses were done by using the software package Sigma Stat 2.0 (SPSS Inc.).

3. Results

3.1. Experimental Results. Captured images at distension pressures of 0.0, 0.2, and 0.4 kPa are shown in Figure 2(a). As the larger section of the sample tended to collapse beyond the viewing field of the cameras, only the patch marked with colour (Figures 2(b) and 2(c)) was analyzed. The colour graphics in Figures 2(b) and 2(c) represent the measured full-field strain distribution from DIC measurement. The stomach surface was distended with outwards displacement in ranges 0.51, 1.67 with mean value 0.95 ± 0.14, 1.12, 2.46 with mean value 1.72 ± 0.25 and 2.17, 4.67 with mean value 3.39 ± 0.51 mm in pressures 0.2, 0.4, and 0.6 kPa. Representative surface displacement, calculated from each correspondence surface point pairs, at distension pressure of 0.4 kPa showed a nonhomogeneous surface displacement on the detected stomach surface patches. The surface at the bottom displaced more than the rest of stomach patch (Figure 2(d)).

3.2. Accuracy of the SC Method-Based Calculations. The colour marked surface in Figure 2 was estimated using the SC method by matching the surface at the reference state (reference surface) to the distended state (target surface). For RS 1, that is, the same surface sample counts between the reference

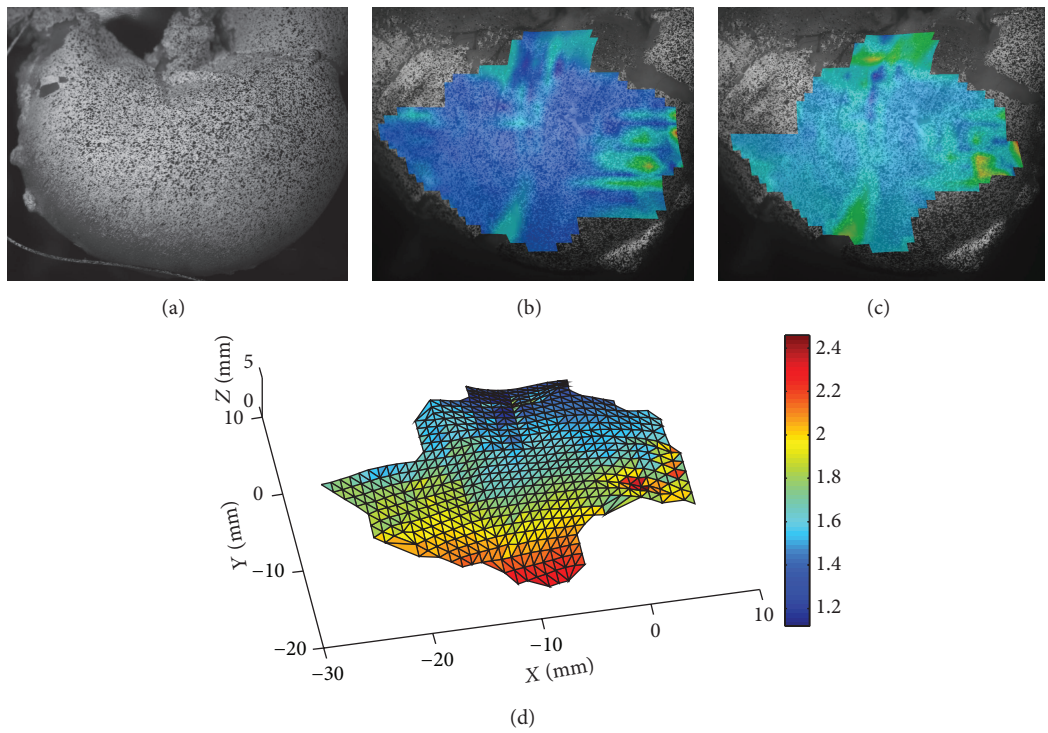

Figure 2: The stomach surface at distension pressure of 0.0 kPa (a), 0.2 kPa (b), 0.4 kPa (c), and the calculated 3D displacement distribution at pressure 0.4 kpa (d). The colour areas in figures (b) and (c) are DIC measured full-field strain distributions where images were obtained from the DIC system. The displacement distribution in (d) was calculated from (1), by using the DIC system recorded 3D coordinates of each correspondence surface point pairs between the reference surface (pressure = 0.0 kPa) and the target surface (pressure = 0.4 kPa). Colours from blue to red represent increasing values.

Table 1: Errors between the SD method calculation and DIC measurement.

Pressure/ε	RS 1 (Nr = Nt)	RS 2 (Nr = 90% × Nt)	RS 3 (Nr = 80% × Nt)
0.2 kPa	5% ± 8%	7% ± 15%	7% ± 12%
0.4 kPa	7% ± 11%	11% ± 16%	14% ± 18%
0.6 kPa	8% ± 11%	22% ± 19%	23% ± 20%

Notes: data are means ± SD; RS 1, RS 2, and RS 3: the reference surfaces 1, 2, and 3; Nr: the surface sample counts on the reference surface (surface at pressure = 0.0 kPa); and Nt: the surface sampling point on the DIC measured target surface (surface at pressures 0.2, 0.4, or 0.6 kPa).

surface and the target surface, the SC method calculated correspondence surface agreed well with the DIC measurement at all three pressure levels (Figure 3(a), Table 1). For RSs 2 and 3, increased pressure and surface sample counts differences resulted in bigger errors between the target surface and the correspondence surface (for factor 1 = pressure, $F = 197.1$, $P < 0.001$ and for factor 2 = different surface sample counts, $F = 127.04$, $P < 0.001$, Figure 3(b), Table 1). However, for pressure 0.2 kPa, the increased surface sample count difference likely did not affect the accuracy of the calculation.

4. Discussion

To the best of our knowledge, this is the first study to validate the 3D SC-based image registration method using a unique tracking features measurement. The accuracy of the SC method-based image registration was described by comparing the calculated 3D correspondence surface to the DIC measurement. Compared with previous validation studies on the SC method, we moved a step further by comparing the shape similarity between the target surface and correspondence surface for each single surface point. Hence we described quantitatively the accuracy of the SC calculations.

Exploration of disease-induced tissue remodelling in visceral organs will be improved dramatically by the introduction of medical imaging modalities such as Magnetic Resonance Imaging (MRI) and ultrasonography. The use of medical image derived, 3D-reconstructed numerical models needs further development in the photogrammetry-based tissue remodelling analysis. Previous studies have demonstrated associations between morphometric and kinematical abnormalities and diseases in visceral organs such as heart, lungs, and stomach [6, 13–19]. Our recent study demonstrated the feasibility to describe the kinematic activity of visceral organs by using combined SC-based nonrigid registration and full-field strain analysis. However, a limitation of SC method-based point matching was, because of global and local dissimilarity and existence of outliers, the significant amount of point mismatching occurring between the correspondence surface and the target surface. Visceral organs, such as stomach and bladder, undergo nonlinear and large deformation under physiological condition. For example, the volume of the stomach can be changed manifolds from empty

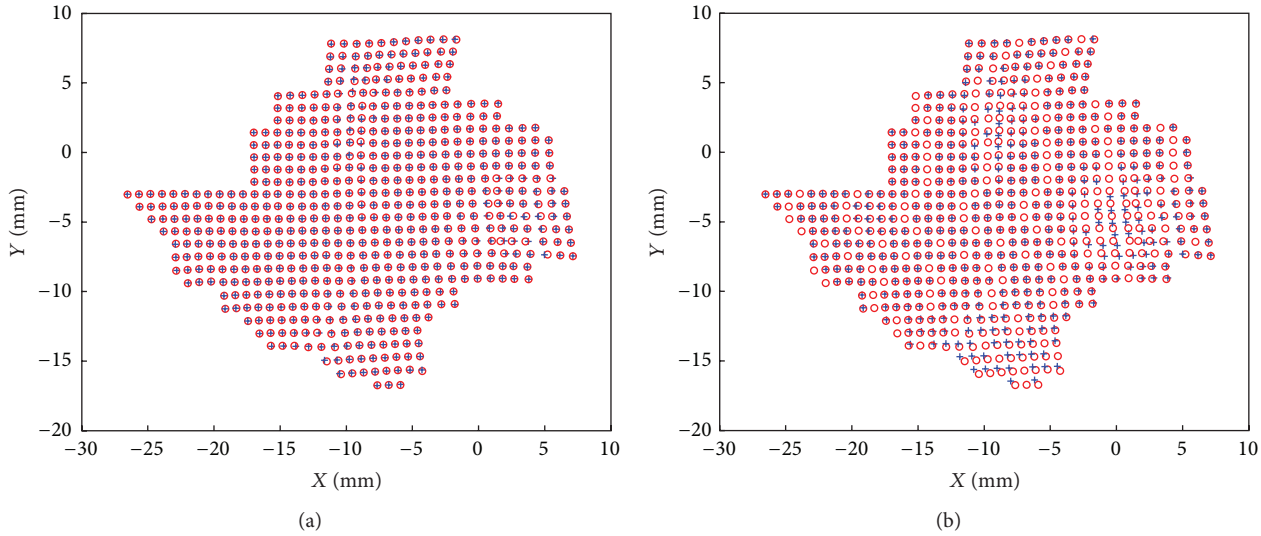

Figure 3: A representative DIC measured target surface (empty circles) and the SC method calculated correspondence surface (crosses) at pressure 0.4 kPa with the RS 1 (a) and RS 3 (b) for the SC calculation. The calculated corresponding surface with RS 1 showed a good agreement with the target surface. However, there are some surface points mismatching when the RS 3 was selected. RS 1, the reference surface that was detected by DIC measurement at pressure 0 kPa, and the RS 3, the same surface as the reference surface 1, but resampling with 80% surface sample counts of the RS 1 (selecting four surface points in every five surface points). Target surface, the surface measured by DIC at pressure 0.4 kPa.

to full. Moreover, heterogeneous distribution of the organ wall material will enhance deformation that caused local shape variation. Hence, using nonlinear image registration methods on living organs to define associations between the kinematical properties, tissue remodelling and diseases, it is important to determine the degree of how the method is an accurate representation of the real world from the perspective of the intended uses of the method [20].

Analysis in this study showed that the reference surface and the target surface with larger shape similarity had a better accuracy for surface point matching. Furthermore, a lower resolution of the reference surface (i.e., the reference surface has less surface sample count compared with that in the target surface) enlarges the error for the surface matching. Hence, matching between two large deformed surfaces should be achieved by a number of monotonic deformation paths, that is, by using the incremental deformation analysis. The errors caused due to the lower resolution of the reference surface can be improved in our near future studies by using soft assignments [5] or the soft shape context method [21]. This will allow multi-samples in the target surface to be assigned to one sample in the reference surface and hence will be more robust to distortions and the surfaces with different sample counts.

Some surface points with noncontinuous displacement were found in the DIC measurement (Figure 2(d)). Noncontinuous displacement could occur when some markers moved out of the gastric surface during the distension. However, the DIC system is limited in the fixed camera setting and thus resulting in loss of information and potentially increased measurement error on the surface points with those moved markers [12]. In this study, only a part of the stomach surface patch was captured by the DIC system. However, the surface patch covered the stomach body including the lesser and the great curvatures, where the major features of the distension that caused stomach deformation were represented [22]. Further studies with larger view scale on 3D measurement are needed for testing the whole 3D surface. Rotation invariance is not considered in this work as data sets are already in a similar position and orientation.

In conclusion, this is the first study to validate the 3D SC-based image registration method by using unique tracking features measurement. The influence of the shape similarity and the resolutions of the reference surface to the accuracy of point-by-point correspondence between two surfaces were investigated. Combination of the presented method and the recently developed combined SC and full-field strain analysis method will pave a way in the future to define the association between tissue remodelling and disease in more detail and will help to build a patient-based quantitative model for accessing disease induced remodelling *in vivo*.

Appendices

A. Point Matching

The shape context of a point is a measure of the distribution of relative positions with other points. The distribution is defined as a joint histogram where each histogram axis represents a parameter in a polar coordinate system. For a P on the shape, the histogram of the relative coordinates of the remaining N-1 points is defined to be the shape context of P. In a 3D shape context, a point histogram is built based on a 3D spherical coordinate system. For any two points (P_m and q_n) in different configurations, P_m belonging to point set

1 (reference state) and q_n belonging to point set 2 (deformed state), a measure of similarity between these two points can be computed as

$$C(p_m, q_n) = C_{mn} = \frac{1}{2}\sum_{l=1}^{L}\frac{\left(h_m(l) - h_n(l)\right)^2}{h_m(l) + h_n(l)}, \quad (A.1)$$

where $h_m(l)$ and $h_n(l), l = 1, 2, \ldots L$ denote the L-bin normalized histogram (shape context) of P_m and q_n, $C(P_m, q_n) = C_{mn}$ is the cost of matching these two points. Therefore, a low cost value for two shape contexts means a high similarity between the two points.

On the basis of the previous description of (A.1), a cost matrix between all pairs of points P_m on the first shape and q_n on the second shape can be defined. Hence, the points in the first shape that best resembles the associate set of points in the second shape can be obtained by minimizing the total corresponding cost as

$$H = \min \sum_{\forall m,n} C_{mn}. \quad (A.2)$$

The Hungarian method was used to minimize the cost function and enforce a one-to-one point matching. After completing the one-to-one matching search, the points which are set with high similarity are chosen as final correspondences.

B. Nonrigid Registration

On the basis of the points matching procedure described above, high similarity point pairs between the reference shape and the deformed shape were identified. For finding the entire matched points in these two shapes, the identified point pairs were used as a resource for the registration by mapping the entire points from the first configuration to the second configuration with a thin-plate spline method (TPS) [23]. The TPS model, describing a transformed 3D point (x', y', z') independently as a function of a source point (x, y, z), can be expressed as

$$\begin{aligned}\left(x', y', z'\right) &= \left(f_x(x, y, z), f_y(x, y, z), f_z(x, y, z)\right),\\ f(x, y, z) &= a_1 + a_2 x + a_3 y + a_4 z\\ &\quad + \sum w_i U\left(\left|P_i - (x, y, z)\right|\right),\end{aligned} \quad (B.1)$$

where $U(r) = r^2 \log r$ is the kernel function and r is Euclidean-distance between 2 points. P_i $(i = 1, 2, \ldots, N)$ are points in the first shape; N is the total points number in the first shape. $a = \{a_1, a_2, a_3, a_4\}$ is the global affine coefficients of the transformation and $w = \{w_1, \ldots, w_n\}$ is the coefficients of the additional nonlinear deformation. The identified corresponding points are used to compute the coefficients of the TPS function by minimizing its bending energy as

$$E[f] = \iiint f\left|D^2 f\right|^2 dX, \quad (B.2)$$

where $D^2 f$ is the matrix of second-order partial derivatives of f and $|D^2 f|^2$ is the sum of squares of the matrix entries. $dX = dx, dy, dz$.

With the obtained TPS function, a nonrigid wrap can thus be applied to the entire point of the referenced shape, and the registered deformed shape can be obtained with a smooth deformation field. For reducing the point mismatching in shape context analysis, the developed topological structure correction method (TSCM) [8] was used in this study.

Conflict of Interests

The authors declare that there is no conflict of interests regarding the publication of this paper.

Acknowledgment

The study was supported by grants from Karen Elise Jensens Foundation.

References

[1] O. Acosta, J. Fripp, V. Doré et al., "Cortical surface mapping using topology correction, partial flattening and 3D shape context-based non-rigid registration for use in quantifying atrophy in Alzheimer's disease," *Journal of Neuroscience Methods*, vol. 205, no. 1, pp. 96–109, 2012.

[2] J. Carballido-Gamio, J. S. Bauer, R. Stahl et al., "Inter-subject comparison of MRI knee cartilage thickness," *Medical Image Analysis*, vol. 12, no. 2, pp. 120–135, 2008.

[3] O. Acosta, J. Fripp, A. Rueda et al., "3D shape context surface registration for cortical mapping," in *Proceedings of the 7th IEEE International Symposium on Biomedical Imaging: From Nano to Macro (ISBI '10)*, pp. 1021–1024, April 2010.

[4] S. Belongie, J. Malik, and J. Puzicha, "Shape matching and object recognition using shape contexts," *IEEE Transactions on Pattern Analysis and Machine Intelligence*, vol. 24, no. 4, pp. 509–522, 2002.

[5] M. Kortgen, G. Park, M. Novotni et al., "3D shape matching with 3D shape contexts," in *Proceedings of the 7th Central European Seminar on Computer Graphics*, Budmerice, Slovakia, 2003.

[6] M. Urschler and H. Bischof, *Matching 3D Lung Surfaces with the Shape Context Approach*, 2004.

[7] M. Urschler and H. Bischof, "Assessing breathing motion by shape matching of lung and diaphragm surfaces," in *Medical Imaging 2005: Physiology, Function, and Structure from Medical Images*, Proceedings of SPIE, pp. 440–452, February 2005.

[8] D. Xiao, D. Zahra, P. Bourgeat et al., "An improved 3D shape context based non-rigid registration method and its application to small animal skeletons registration," *Computerized Medical Imaging and Graphics*, vol. 34, no. 4, pp. 321–332, 2010.

[9] D. Liao, J. Zhao, and H. Gregersen, "A novel 3D shape context method based strain analysis on a rat stomach model," *Journal of Biomechanics*, vol. 45, pp. 1566–1573, 2012.

[10] M. A. Sutton and J. Orteu, "Digital image correlation (DIC)," in *Image Correlation for Shape, Motion and Deformation Measurements*, H. Schreier and J. Jomas, Eds., Springer, New York, NY, USA, 2009.

[11] J. Tyson, T. Schmidt, and K. Galanulis, "Biomechanics deformation and strain measurements with 3D image correlation

photogrammetry," *Experimental Techniques*, vol. 26, no. 5, pp. 39–42, 2002.

[12] M. A. Sutton, "Digital image correlation for shape and deformation measurements," in *Springer Handbook of Experimental Solid Mechanics*, pp. 565–600, Springer, New York, NY, USA, 2008.

[13] E. Distrutti, F. Azpiroz, A. Soldevilla, and J.-R. Malagelada, "Gastric wall tension determines perception of gastric distention," *Gastroenterology*, vol. 116, no. 5, pp. 1035–1042, 1999.

[14] D. Liao, J. B. Frøkjær, J. Yang et al., "Three-dimensional surface model analysis in the gastrointestinal tract," *World Journal of Gastroenterology*, vol. 12, no. 19, pp. 2870–2875, 2006.

[15] H. Liu, H. Hu, C. L. Ken Wong, and P. Shi, "Cardiac motion analysis using nonlinear biomechanical constraints," in *Proceedings of the 27th Annual International Conference of the Engineering in Medicine and Biology Society*, vol. 2, pp. 1578–1581, 2005.

[16] G. Moragas, F. Azpiroz, J. Pavia, and J.-R. Malagelada, "Relations among intragastric pressure, postcibal perception, and gastric emptying," *American Journal of Physiology—Gastrointestinal and Liver Physiology*, vol. 264, no. 6, pp. G1112–G1117, 1993.

[17] X. Papademetris, A. J. Sinusas, D. P. Dione, and J. S. Duncan, "Estimation of 3D left ventricular deformation from echocardiography," *Medical Image Analysis*, vol. 5, no. 1, pp. 17–28, 2001.

[18] K. Schulze-Delrieu and S. S. Shirazi, "Pressure and length adaptations in isolated cat stomach," *American Journal of Physiology—Gastrointestinal and Liver Physiology*, vol. 252, no. 1, part 1, pp. G92–G99, 1987.

[19] P. Shi, A. J. Sinusas, R. T. Constable, and J. S. Duncan, "Volumetric deformation analysis using mechanics-based data fusion: applications in cardiac motion recovery," *International Journal of Computer Vision*, vol. 35, no. 1, pp. 87–107, 1999.

[20] H. B. Henninger, S. P. Reese, A. E. Anderson, and J. A. Weiss, "Validation of computational models in biomechanics," *Journal of Engineering in Medicine*, vol. 224, no. 7, pp. 801–812, 2010.

[21] D. Liu and T. Chen, "Soft shape context for iterative closest point registration," in *Proceedings of the International Conference on Image Processing (ICIP '04)*, pp. 1081–1084, October 2004.

[22] D. Liao, J. Zhao, and H. Gregersen, "Regional surface geometry of the rat stomach based on three-dimensional curvature analysis," *Physics in Medicine and Biology*, vol. 50, no. 2, pp. 231–246, 2005.

[23] F. L. Bookstein, "Principal warps: thin-plate splines and the decomposition of deformations," *IEEE Transactions on Pattern Analysis and Machine Intelligence*, vol. v, pp. 567–585, 1992.